Measurement of local creep properties in stainless steel welds

Conference or Workshop Item

Creep Deformation Measurement of 316H Stainless Steel Multi-pass Welded Joints using Digital Image Correlation

Y. Sakanashi*, S. Gungor and P. J. Bouchard

Materials Engineering
The Open University, Walton Hall
Milton Keynes MK7 6AA, UK

*Corresponding author: yuki.sakanashi@open.ac.uk

ABSTRACT

A high temperature measurement system for creep deformation based on the digital image correlation (DIC) technique is described. The new system is applied to study the behaviour of a multi-pass welded joint in a high temperature tensile test and a load controlled creep test at 545°C. Spatially resolved tensile properties and time dependent creep deformation properties across a thick section type 316 stainless steel multi-pass welded joint are presented and discussed. Significantly lower creep strain rates are observed in the HAZ than in the parent material which is attributed to the introduction of substantial plastic strain in the parent material on initial loading. The weld metal shows the fastest creep rates and a variation that appears to correlate with individual weld passes. The visual information provides not only the local creep strain distribution but also the reduction of area and true stress distribution based on strains measured in the transverse direction. The results demonstrate the capability of the DIC technique for full field measurement of displacement and strain at high temperature long term creep tests.

INTRODUCTION

The life of steam pipework systems in power plants operating at high temperatures and pressures is largely governed by the integrity of the welded regions. Assessment of the structural integrity of these systems requires knowledge of time-dependent creep deformation in and around the welded joints at the operating temperatures. The secondary strain rate is a good indicator of the accumulation of creep strain and therefore this has been used widely in ductility exhaustion based assessments of plant lifetime. However, the creep behaviour of a multi-pass welded joint is complicated it being influenced by variations in microstructure and the thermo-mechanical history of the welding process. The conventional method of measuring the variation of creep properties in a weldment is to cut small samples from the weld, the heat affected zone (HAZ) and parent material and carry out individual creep tests in which the strain response of the test sample with time is measured using extensometers or high temperature strain gauges [1,2]. Such deformation data have been incorporated into finite element creep simulation analyses of multi-pass welded joints by many researchers [3-8]. However, it may not be feasible to extract reasonably sized test samples from the required regions if the weldment is not sufficiently large. Moreover, it may be argued that due to the change in constraint conditions, the behaviour of samples extracted from the weldment will be different from the behaviour of the same material in situ. Hongo et al [9] successfully developed a system based on a moiré interferometry technique to measure the creep strain distribution in a thick welded joint but this required tedious specimen preparation and interruption during the creep tests. Recently the present authors have demonstrated the use of a digital image correlation (DIC) technique for the measurement of strain during tensile and creep tests at elevated temperatures [10]. The present article reports measurements of local creep properties in a thick section multi-pass weldment.

HIGH TEMPERATURE DIC SYSTEM

The DIC technique has been successfully employed by many researchers to map the strain variation spanning cross-weld specimens during room temperature tensile tests [11-15]. The working principle of DIC is based on sophisticated computational algorithms that track the grey value patterns in digital images of the test surfaces, taken before and after a loading event that produces surface deformations [16]. Lyons *et al* [17] were the first to demonstrate the capability of DIC to measure strains at high temperatures. They measured free thermal expansion and strains due to tensile loads on Inconel 718 superalloy specimens at temperatures up to 650°C.

It is essential to have an adequate speckle pattern for accurate measurement of strain using DIC. However, during high temperature tests, the image contrast deteriorates quickly due to oxidation. In the present study, the surface of the specimens were coated with a silicon ceramic based paint (VHT FlameProof™) which provided a non-degrading appearance. Two different colours, black and white spray were applied to obtain a random speckle pattern and the specimens were cured three times before the experiment. Figure 1 shows the speckle pattern on the specimen surface after 6 weeks at 600°C.

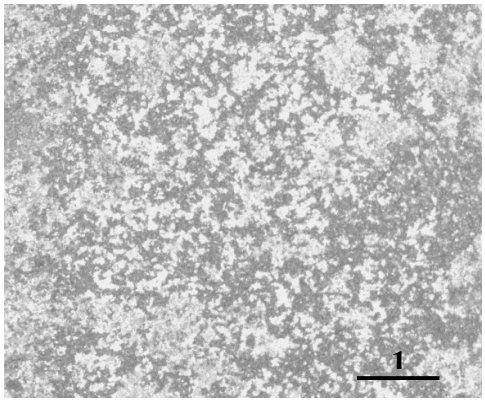

Fig. 1. Appearance of the surface coating after 6 weeks at 600ºC.

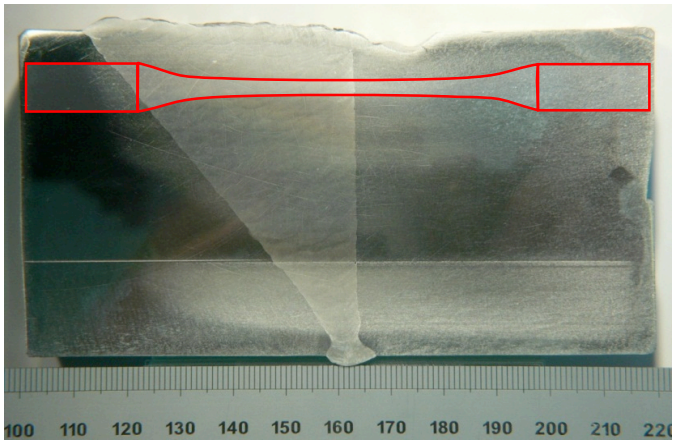

Fig. 2 Photograph of the AISI Type 316H stainless steel thick section weldment indicating the location and geometry of the cross-weld creep test specimen.

EXPERIMENTAL

Material

The material used in this study was extracted from an AISI Type 316H austenitic stainless steel cylindrical butt weld of outer diameter 430mm and 65mm wall thickness (Figure 2). The weld was made using a manual metal arc process with 129 passes deposited in 26 layers starting at the root. The hardness map given in Figure 3(a) clearly shows the location of the weld metal which has higher yield strength. Figure 3(b) shows the variation in hardness along the top-thickness line of the weldment at 10 mm from the top face. The parent material hardness is approximately constant (170 HV) at distances greater than about 12 mm from the weld fusion boundary. In the heat affected zone region (<12mm from the fusion boundary) the hardness increases to match the higher hardness (approx 220 HV) in the weld metal. The hardness in the weld metal appears to be correlated with individual multi weld passes.

Tensile and creep specimens were cut from cylindrical blanks extracted from the weldment using electro-discharge machining (EDM). The gauge lengths of the extracted cross-weld specimens cover approximately one-half of the weld and HAZ, as shown in Figure 3. The ends of the specimens had M12 threads for fixing into the testing machine. The gauge length was machined flat to give a cross-section 6mm wide by 3mm thick in order to provide a surface suitable for DIC measurement.

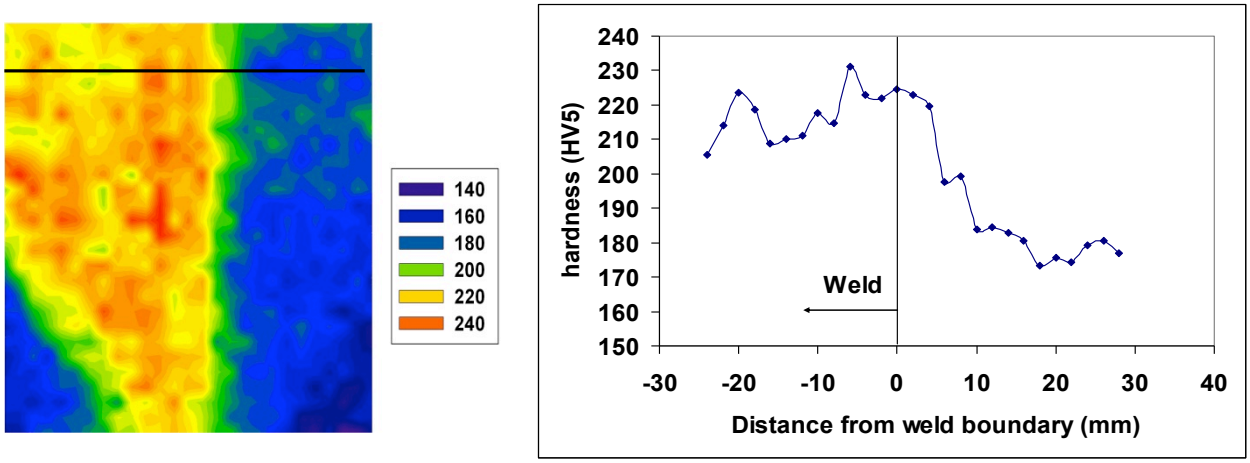

Fig. 3 (a) Vickers hardness map of the weldment (left), and **(b)** the variation of hardness across the mid-thickness line shown in (a) corresponding to the gauge length of the test specimen (right).

Tensile and creep test

A high temperature tensile test was carried out to investigate the tensile properties of this sample at 545°C. An Instron slow-strain rate screw-driven testing machine was used for this experiment. The specimen was heated overnight at 545°C then a test was executed with an extension rate of 0.1mm/min. Images were taken at 10 second intervals in the elastic region, then at 40 second intervals during plastic deformation.

The creep test was carried out at 545°C. Figure 4 shows the DIC high temperature creep deformation measurement system. A three-zone furnace was specially manufactured with a porthole side through its wall for the purpose of imaging the sample surface during testing. The field of view of the specimen by the camera is restricted by the dimensions of the opening (window), which is 20 mm by 40 mm. The specimen is placed in the middle of the furnace and vertically aligned to give the required view of gauge section by the camera. The specimen was subjected to a constant load, which gave an initial stress of 315 MPa. A digital SLR camera with a 200 mm focal length macro lens was used to photograph the gauge section of the specimen. Images of the specimen surface during testing were acquired at regular intervals using time-lapse photography software.

The specimen surface was illuminated using a fibre optic light bundle, which was coupled to a strobe flash unit triggered by the digital camera. It was found that this set up provided adequate illumination and the images obtained were of good contrast (Figure 5). The specimen was fixed into the loading frame using a screw joint inside the furnace and two thermocouples were attached to the specimen at the top and bottom of the specimen, beyond the gauge length, using drilled small holes.

DIC analysis procedure

An important parameter in the DIC analysis is the speckle size. If the speckle size is too large, the subset size can be increased to achieve accurate correlation, however, increasing the subset size reduces the spatial resolution [19]. The imaging system was set up to give a pixel size of about 10 μm and the corresponding speckle size was approximately 50 μm, which was found to give good correlation in the DIC analysis.

Images were acquired at 1 hour intervals after the specimen was heated to the test temperature (545°C) and the load was applied (315 MPa). The images were recorded in uncompressed raw format in the camera and then converted to 8 bit grayscale using commercial software. The converted images were imported into commercial DIC software [18] for processing. The procedure for analysing the images is described in [15]. Briefly, the imported images were first corrected for rigid body rotations and the gauge area was extracted from the camera image to calculate the full field of the displacement map and strain distribution. The extracted work space was divided into small subsets called interrogation windows and a cross-correlation algorithm was applied to each window. Once the algorithm detected the next window position (deformed subset position), the displacement vector was determined by distance between each subset centre point. The appropriate parameter settings were selected: multi-pass, decreasing window size started 128 × 128 pixels with 50%, two iterations overlap then 64 × 64 pixel with 6 iterations for the tests carried out in this study. The displacement results calculated by the DIC software were exported into the general purpose analysis software Matlab to determine strains by differentiating seven

point displacement data as this approach has been found to give results that correlate most closely with finite element results [15]. The strain values reported in this study were averaged across the width sections of the specimen gauges in order to highlight the strain variation across the different zones of the weldment along the gauge length.

Fig. 4 DIC high temperature creep measurement system

Fig. 6 The ruptured tensile specimen tested at 545ºC.

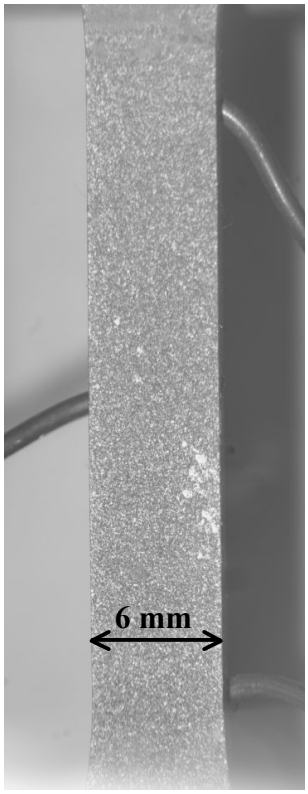

Fig. 5 An example image of the test specimen obtained by the DIC system at 545ºC

RESULTS

High temperature tensile test

The tensile test specimen was loaded until fracture, which occurred in the weld metal (Figure 6). The strain was averaged across the width of the specimen and the evolution of the strain variation along the gauge length obtained. Figure 7 shows the strain variation along the gauge length of the specimen at 315 MPa, which was the loading level for the creep test. It can be seen that the strain in the HAZ is considerably smaller relative to the weld and parent metal. A strain fluctuation within the weld metal zone due to weld passes can be observed.

Local stress-strain curves were constructed for each subset. Figure 8 shows stress-strain curves of parent, HAZ and weld at 545ºC. The sampling positions for the curves are x=10mm, x=2.5mm and x=–2.5mm from the weld boundary, respectively. The results show that the yield stress of parent metal is considerably smaller than the weld metal and the HAZ. A linear line was fitted to the elastic region of each local stress-strain curve and used to determine the 0.2% yield stress at each location. The 0.2% proof stress variation along the cross-weld specimen is shown in Figure 9 and agrees well with the hardness variation. The weld metal zone has about 80 MPa higher proof stress compared with the parent metal. DIC also provides information about the transverse strain across the gauge section. The variation in the reduction of area (RA) was calculated on the assumption that the transverse strain across the width of the gauge is the same as the transverse strain through the thickness of the gauge. The variation of RA along the gauge section of the specimen at a stress of 315MPa is shown in Figure 10. It can be seen that the parent has large RA due to its higher ductility and that the RA gets larger moving from the weld boundary to the centre of the weld. It was observed that within the weld metal, the RA peaked in the middle of the weld pass layers.

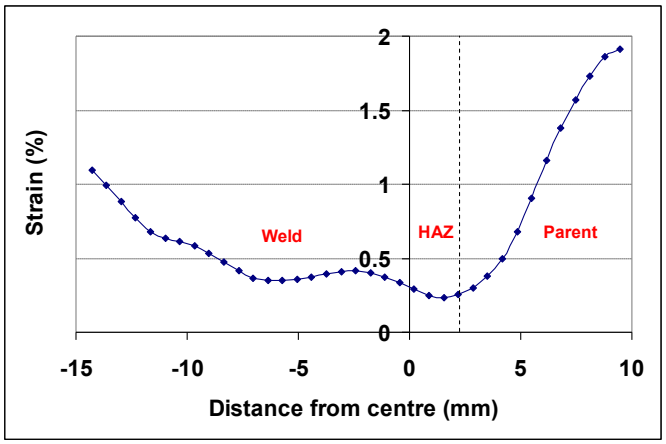

Fig. 7 Instantaneous strain distribution along the cross-weld tensile specimen under tensile load of 315 MPa at 545ºC.

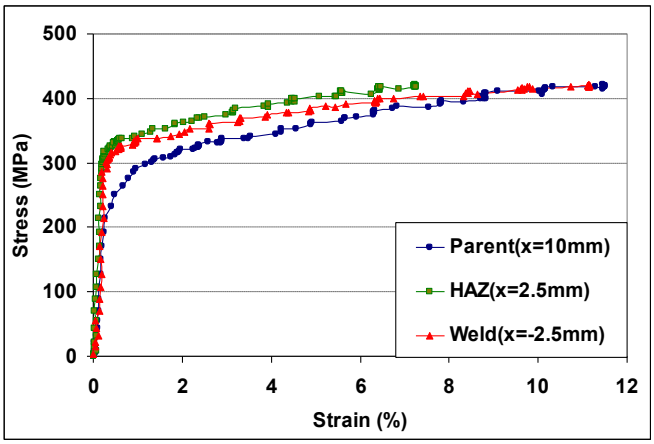

Fig. 8 Tensile test stress-strain curves for parent material (x=10mm), HAZ (x=2.5mm) and Weld (x=-2.5mm) at 545ºC

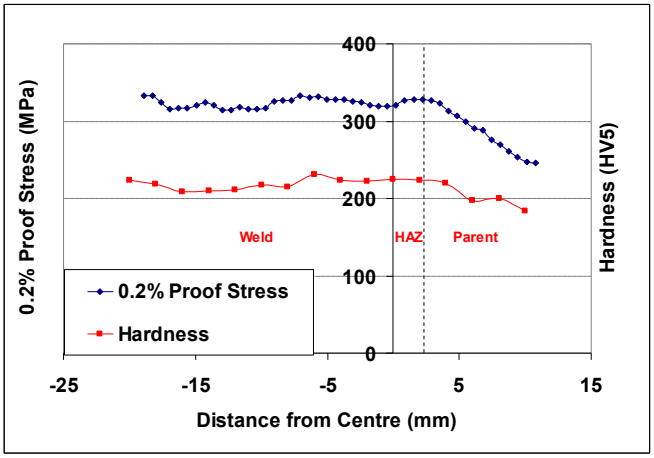

Fig. 9 Measured 0.2% proof stress variation along the cross-weld specimen gauge length at 545°C, and room temperature as-welded hardness variation across the weldment.

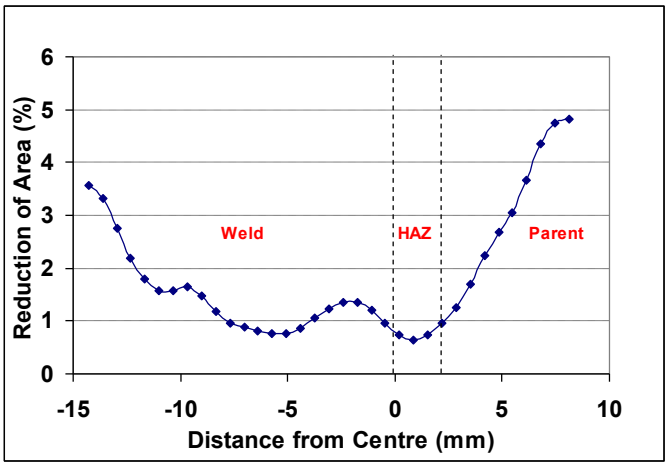

Fig. 10 Reduction of area along the cross-weld specimen gauge length (based on measured change of width) under tensile load of 315 MPa at 545°C.

Creep test

At the time of the writing, the test had undergone 1250 hours without rupture. The acquired images were analysed over this test duration. Figure 11 shows the strain evolution along the gauge length of the specimen at different times. Parent, HAZ and weld metal zones show different creep deformation behaviour clearly. Although the high temperature tensile test indicated that parent accumulated the largest strain, here the weld metal zone is seen to be accumulating larger creep strain than the parent material. The creep strain increases from the first pass of the weld (centre of specimen) towards the outer transverse layers of the weld. Figure 12 is a photograph of the multi-pass layer of weld, which was cut from the side of specimen gauge length to create flat sides. As shown in this photograph, the weld metal zone has a complicated multi-pass pattern, however, the width of each pass layer is approximately 6mm. The creep strain variation corresponds to the spatial disposition of the weld passes with the middle region of each weld bead showing larger creep strain than the weld bead boundary. In addition, it is noticeable that the creep strain developing in the HAZ is considerably smaller than that accumulating in the parent metal and weld metal.

Local creep deformation curves corresponding to different three spatial positions: parent metal (x=10mm from the weld boundary), HAZ (x=2.5mm) and weld (x=–2.5mm) are shown in Figure 13. The HAZ is creep-strong relative to the parent and the weld materials. Although the instantaneous strain of the parent metal was large in the high temperature tensile test (Figure 7), the creep strain in the weld metal is observed to be higher than in the parent metal. This is partly because the yield stress of the parent metal is significantly smaller than the applied nominal stress of 315MPa which roughly corresponds to the yield strength of the HAZ and the weld (see Figure 9).

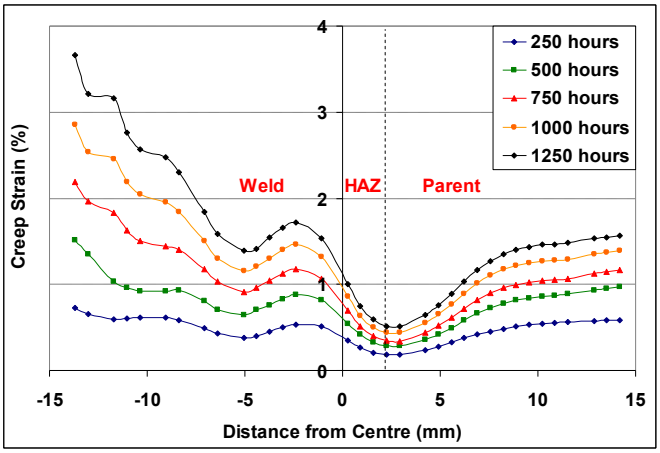

Fig. 11 Measured variation in creep strain along the cross-weld creep specimen as a function of exposure time, under an applied stress of 315 MPa at 545ºC.

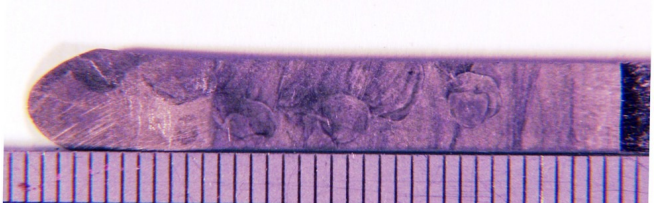

Fig. 12 Photograph showing weld passes in test specimen.

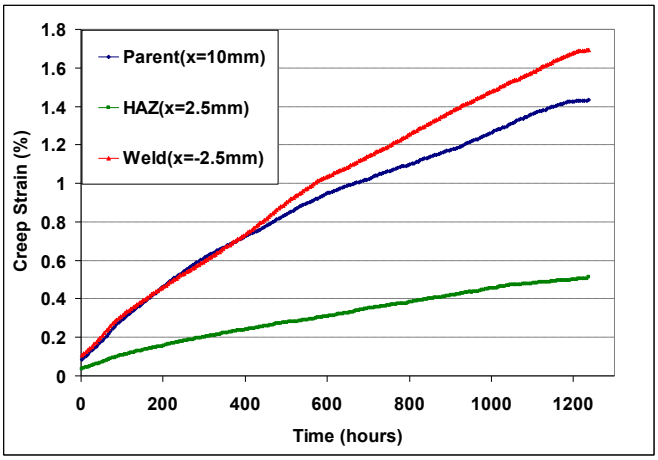

Fig. 13 Local creep curves of Parent (x=10mm), HAZ (x=2.5mm) and Weld (x=-2.5mm) materials

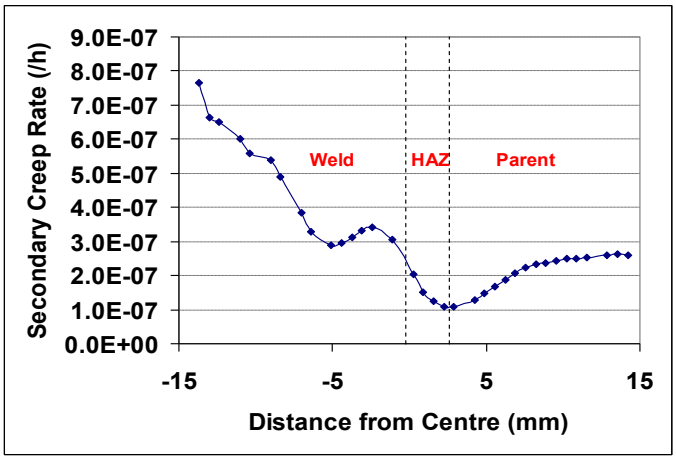

Fig. 14 Secondary creep rate distribution along the cross-weld test specimen under applied load of 315 MPa at 545ºC

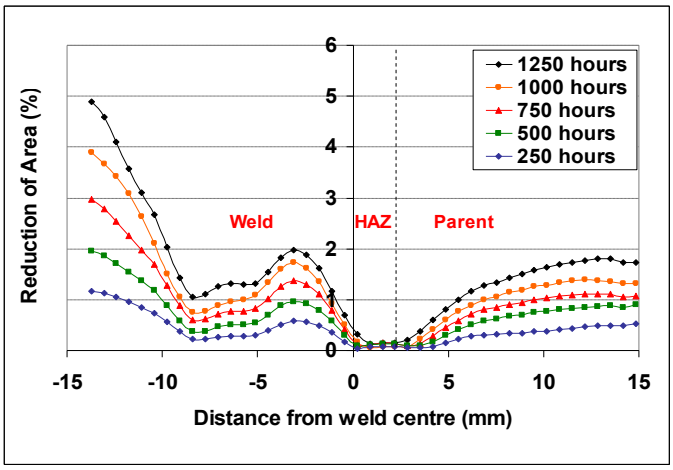

Fig. 15 Reduction of area distribution across the cross-weld specimen based on specimen width direction data.

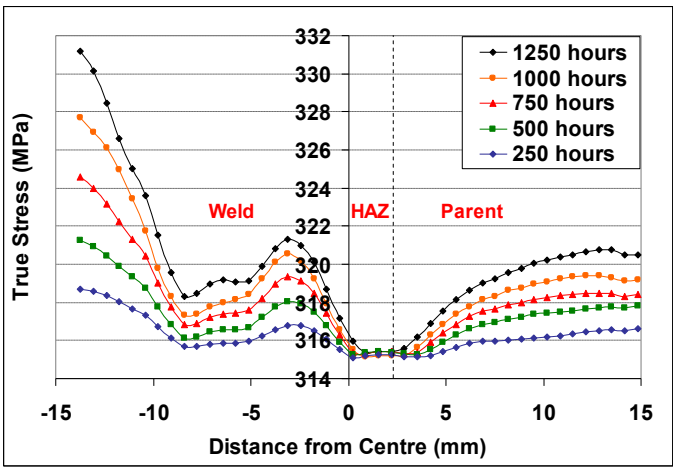

Fig. 16 True stress distribution across the cross-weld specimen based on change in specimen width data.

Upon applying the load at the beginning of the creep test, a large amount of plastic strain occurred in the parent material which seems to have caused work hardening. After the creep test started, the material properties and the ductility of the parent changed due to this work hardening, thus the creep strain of the parent metal became smaller than that of the weld zone. On the other hand, the weld metal and the HAZ had a slightly higher initial 0.2% proof stress than the constant applied stress (315MPa), thus initial plastic strain was not introduced during loading process.

Figure 14 shows the secondary creep rate distribution along the gauge length of the cross-weld specimen. The results indicate that the HAZ has the highest creep strength and that the creep rate of both the weld metal and parent material increases with increasing distance from the weld fusion line. It may well be that the variation in weld creep properties correlates with the weld deposition sequence, that is the local thermo-mechanical weld history.

The variations in reduction of area and true stress along the specimen at different creep times are shown in Figure 15 and 16. The data were obtained, similar to the tensile test, on the assumption that the strain through the thickness is the same as the measured transverse strain across the gauge width. The RA and and hence true stress in the HAZ is significantly lower than the other regions once they have started to accumulate creep strain (see Figures 15 and 16). However, the true stress of parent increases to more than 320MPa at 1250 hours and the outermost weld pass rises up to more than 330MPa at the same time. By knowing the true stress distribution along the cross-weld sample, we can estimate the stress change with time and potentially take account of its effect on creep deformation.

CONCLUSIONS

A high temperature deformation measurement system with digital image correlation has been developed and applied to study the behaviour of a multi-pass welded joint in a high temperature tensile test and a load controlled creep test at 545°C. The technique successfully produced spatially resolved tensile properties and time dependent creep properties across a thick section type 316 stainless steel multi-pass welded joint. Significantly lower creep strain rates were observed in the HAZ than in the parent material. It was noted, from the high temperature tensile test, that the parent material would have undergone substantial plastic strain on initial loading in the creep test whereas the response of the HAZ and weld metal response would have been elastic. The weld metal showed the fastest creep rates and a variation that correlated with individual weld passes. Interestingly the creep properties appeared to be higher in the central region of a weld bead that at the weld bead boundaries. There also appeared to be a systematic increase in creep strain rate moving laterally away from the fusion boundary suggesting a correlation with the original weld deposition sequence. The visual information provides not only the local creep strain distribution but also the reduction of area and true stress distribution based on strains measured in the transverse direction. The results demonstrate the capability of the DIC technique for full field measurement of displacement and strain at high temperature long term creep tests.

ACKNOWLEDGEMENTS

The authors would like to thank EDF Energy for providing the welded sample and funding the research.

REFERENCES

[1] Hiromichi Hongo, Masayoshi Yamazaki, Takashi Watanabe, Junichi Kinigawa, Tatsuhiko Tanabe, Yoshio Monma and Takanori Nakazawa “Creep deformation behavior of weld metal and heat affected zone on 316Fr steel thick plate weld joint” Japan society of material science, Vol.48, No.2, pp.116-121 (1999) (in Japanese)

[2] Hiromichi Hongo, Masayoshi Yamazaki, Takashi Watanabe, Tatsuhiko Tanabe, Masaaki Tabuchi and Yoshio Monma “Evaluation for creep properties of 316FR weld metal with miniature weld metal and full-thickness welded joint specimes ” Japan society of material science, Vol.53, No.5, pp.566-571 (2004) (in Japanese)

[3] kenji Nakacho, Yukio Ueda, Junichi Kinugawa and Masayoshi Yamazaki ”Development of a simple model for creep analysis of thick welded joint” Japan welding society Vol.12 No.2 p249-254 (1994) (in Japanese)

[4] Kenji Nakasho and Masayoshi Yamazaki “Estimation of creep life of thick welded joint using a simple model -Creep characteristics in thick welded joint and their improvement (report 2)-“ Japan welding society Vol.19 No.2 p354-359 (2001) (in Japanese)

[5] Junichi Kinugawa, Yoshiki Muramatsu, Yoshio Monma, Masayoshi Yamazaki, Hiromichi Hongo and Takashi Watanabe “Comparison for creep deformation of welded joint of 304 stainless steel by using finite element method” Japan welding society Vol.7 No.1 p117-124 (1989) (in Japanese)

[6] Masayoshi Yamazaki, Yoshio Monma, Hiromichi Hongo, Takashi Watanabe, Junichi Kinugawa and Yoshiki Muramastu “Creep-rupture behavior of butt welded joint of 304 stainless steel thick plate and large specimens” The society of material science, Japan Volume.39 No.440 p509-515 (1990) (in Japanese)
[7] Hiromichi Hongo, Masayoshi Yamazaki, Takashi Watanabe, Masaaki Tabuchi, Tatsuhiko Tanabe and Yoshi Monma “Effect of local Fluctuation of the high temperature strength properties in weld metal deformation behavior of multi-layer welded joint” Japan society of material science, Vol.54, No.2, pp.155-161 (2005) (in Japanese)
[8] Yongui Li, Yoshio Monma, Hiromichi Hongo, Masaaki Tabuchi “Evaluation of creep damage in a welded joint of modified 9Cr-1Mo steel” Journal of nuclear materials 4-5 (2010) 44-49
[9] Hiromichi Hongo, Hirouiki Masuda and Yoshio Monma “Development of simple strain distribution measurement system by interferometry using CCD image elements” The iron and steel institute of Japan, Vol.79 , No.4, p74-79 (1992) (in Japanese)
[10] Sakanashi, Y, Gungor, S and Bouchard, P.J. (2011) “Measurement of Creep Deformation in Stainless Steel Welded Joints” Proc. of the SEM Annual Conference, June 13-16, 2011, Mohegan Sun, Uncasville, Connecticut USA. Also in Optical Measurements, Modeling, and Metrology, Volume 5, Conference Proceedings of the Society for Experimental Mechanics Series, 2011, Volume 9999999, 371-378, DOI: 10.1007/978-1-4614-0228-2_45
[11] Lockwood WD, Tomaz B, and Reynolds AP “Mechanical response of friction stir welded AA2024: experiment and modelling” Materials Sciences and Engineering, A 323, 348-353 (2002)
[12] Sutton MA, Yang B, Reynolds AP and Yan J “Banded microstructure in 2024-T351 and 2524-T351 aluminum friction stir welds: Part II. Mechanical characterization” Materials Sciences and Engineering, A364, 66-74 (2004)
[13] Genevois C, Deschamps A and Vacher P “Comparative study on local and global mechanical properties of 2024 T351, 2024 T6 and 5251 O friction stir welds” Materials Sciences and Engineering, A 415, 162-170 (2006)
[14] Kartal M, Molak R, Turski M, Gungor S, Fitzpatrick ME and Edwards L “Determination of Weld Metal Mechanical Properties Utilising Novel Tensile Testing Methods” Applied Mechanics and Materials, 7-8. pp. 127-132 (2007)
[15] Acar M, Gungor S, Ganguly S, Bouchard PJ, Fitzpatrick ME “Variation of Mechanical Properties in a Multi-pass Weld Measured Using Digital Image Correlation” Proceedings of the SEM Annual Conference, Albuquerque New Mexico USA Society for Experimental Mechanics Inc. (2009)
[16] Sutton MA, McNeill SR, Helm JD and Chao YJ “Advances in two-dimensional and three-dimensional computer vision,” in Topics in Applied Physics, 1st ed., P. K. Rastogi, ed., (Springer, Berlin: Springer) p323-372. (2000)
[17] Lyons JS, Liu J, Sutton MA. High-temperature deformation measurements using digital-image correlation. Experimental Mechanics. 36(1):64-70 (1996).
[18] Strain Master, LaVision GmbH, Anna-Vandenhoek-Ring 19, Gottingen, Germany
[19] Acar, M, Gungor, S, Bouchard, P and Fitzpatrick, M. E. (2010). Effect of prior cold work on the mechanical properties of weldments. In: Proceedings of the 2010 SEM Annual Conference and Exposition on Experimental and Applied Mechanics, 7-10 Jun 2010, Indianapolis, Indiana, USA.